Motion Detection and Adaptation in Crayfish Photoreceptors

A Spatiotemporal Analysis of Linear Movement Sensitivity

RAYMON M. GLANTZ

From the Department of Biochemistry and Cell Biology, Rice University, Houston, Texas 77251

ABSTRACT Impulse and sine wave responses of crayfish photoreceptors were examined to establish the limits and the parameters of linear behavior. These receptors exhibit simple low pass behavior which is well described by the transfer function of a linear resistor–capacitor cascade of three to five stages, each with the same time constant (τ). Additionally, variations in mean light intensity modify τ twofold and the contrast sensitivity by fourfold. The angular sensitivity profile is Gaussian and the acceptance angle (ϕ) increases 3.2-fold with dark adaptation. The responses to moving stripes of positive and negative contrast were measured over a 100-fold velocity range. The amplitude, phase, and waveform of these responses were predicted from the convolution of the receptor's impulse response and angular sensitivity profile. A theoretical calculation based on the convolution of a linear impulse response and a Gaussian sensitivity profile indicates that the sensitivity to variations in stimulus velocity is determined by the ratio ϕ/τ. These two parameters are sufficient to predict the velocity of the half-maximal response over a wide range of ambient illumination levels. Because ϕ and τ vary in parallel during light adaptation, it is inferred that many arthropods can maintain approximately constant velocity sensitivity during large shifts in mean illumination and receptor time constant. The results are discussed relative to other arthropod and vertebrate receptors and the strategies that have evolved for movement detection in varying ambient illumination.

INTRODUCTION

A remarkable feature of many visual systems is their capacity to detect movement (direction and velocity) and target position at the same time and under a wide range of ambient levels of illumination (Buchner, 1984). These abilities place stringent requirements on the photoreceptor array, which must maximize its speed, acuity, and/or sensitivity in the face of competing demands. Receptor dynamics provide a

Address reprint requests to Dr. Raymon M. Glantz, Department of Biochemistry and Cell Biology, Rice University, P. O. Box 1892, Houston, TX 77251.

J. GEN. PHYSIOL. © The Rockefeller University Press · 0022-1295/91/04/0777/21 $2.00
Volume 97 April 1991 777–797

useful starting point for considering these issues. Photoreceptors are piecewise linear systems. When subjected to temporally modulated illumination, the steady-state receptor potential is approximately linear over a wide range of frequencies and modulation depths (DeVoe, 1967; Dodge et al., 1968; Pinter, 1972; Dubs, 1982; Naka et al., 1987). Furthermore, impulse responses are reasonably approximated from the frequency response (DeVoe, 1967; Pinter, 1972). On the other hand, the linear range is generally restricted to responses of a few millivolts (DeVoe, 1967; Knight et al., 1970; Baylor et al., 1974), and changes in the mean level of illumination are associated with changes in sensitivity and time constant (Fuortes and Hodgkin, 1964; Baylor et al., 1974; Naka et al., 1987). These variations reflect functionally important nonlinearities in the visual response, with important implications for movement detection. For these reasons the range and parameters of linear behavior were explored in this study.

A general characteristic of arthropod photoreceptors is that the receptive field can be approximated by a Gaussian sensitivity profile (Wilson, 1975; Dubs, 1982) attributable to the dioptric apparatus (Land, 1984; Smakman et al., 1984). In addition, the receptor potentials do not reveal evidence for neuronal interactions such as lateral inhibition. Thus, in contrast to the *Limulus* eccentric cell (Brodie et al., 1978), the receptor's spatial and temporal transfer functions are mutually independent. In such a system and within the receptor's linear intensity range, the response to a target's translation at any velocity should be related to the product of the receptor's temporal and spatial transfer functions (Brodie et al., 1978; Egelhaaf and Borst, 1989). Changes in the level of light adaptation should alter movement sensitivity through adaptation-dependent variations in the temporal and spatial parameters. In this study, these inferences were examined in receptors maintained in a variety of adaptive states. It was found that variations in receptor time constant and angular sensitivity have substantial and predictable effects on the relationship between target velocity and receptor sensitivity.

In many compound eyes, including those of crayfish, light adaptation produces roughly parallel changes in the acceptance angle and time constant of the photoreceptors. Here it is shown that the detectable velocity range depends on the ratio of the acceptance angle to the time constant. Thus, the variations tend to offset one another so as to minimize the effects of adaptation on the velocity sensitivity profile.

METHODS

Preparation and Recording Procedures

Crayfish, *Procambarus clarkii,* 8–10 cm in length, were exsanguinated at 0–4°C in oxygenated saline. The blood and saline were exchanged through a 1.0-cm^2 opening in the carapace over the pericardial cavity. The eyestalks were cemented to the cephalic carapace with methacrylate. The crayfish was clamped in a plexiglass chamber containing chilled oxygenated saline and maintained at 13°C with a cooling coil. The eye was centered in front of a glass window (1.0 × 2.0 cm) in the wall of the plexiglass chamber. A 0.5-mm opening was made in the dorsal cornea with a sharp scalpel. It was essential to avoid compressing or otherwise distorting the shape of the remaining cornea.

In a few instances indicated in the Results, measurements were made in an isolated eyecup.

The excised eye was mounted on a plexiglass stage in a 50-mm petri dish. Saline was cooled to 13°C with a miniature cooling coil. Receptors remained viable for 3–6 h.

Retinular cells were impaled with micropipettes with tip resistances of 100 MΩ when filled with 2.0 M potassium acetate. Signals were led to a microelectrode amplifier (model 8100; DAGAN Corp., Minneapolis, MN) and electrode capacitance was compensated. Successful impalements yielded membrane resting potentials of 65–75 mV, input resistances of 6–20 MΩ, and peak responses after modest dark adaptation of 30–60 mV. All receptor recordings were stored on an FM tape recorder along with a continuous monitor of the stimulus and a synchronized square wave for periodic stimuli.

The principal light source was a 2-mW helium–neon laser. The 633-nM wavelength is close enough to the 562-nM effective absorption peak of the crayfish principal photopigment (Wald, 1967; Goldsmith, 1978) that an adequate range of intensities was generated. The path of the laser beam contained a spatial filter, a collimating lens, a variable slit, a ferroelectric liquid crystal modulator (Displaytech, Inc., Boulder, CO), an electromagnetic shutter (Uniblitz, Rochester, NY), and a 6.0 log unit neutral density wedge and/or a fixed neutral filter and steering mirrors to control the x and y positions of the beam. A Wild (Heerbrugg, Switzerland) condensing lens (48-mm clear aperture, f 1.0) converted the two-dimensional (x, y) beam deflections into angular deviations focused to the geometric center of the crayfish eye. The stimulus focused on the cornea had the shape of a vertical bar 300 μm in length. In the horizontal dimension the stimulus had a Gaussian intensity profile with a 70-μm half-width. The radiant power was 0.5 mW when the modulator and all neutral filters were removed from the light path. The average unattenuated intensity across the upper half of the Gaussian profile was 18 mW/mm^2. The spatial filter, the steering mirrors, and the Wild condensing lens were mounted on heavy manipulators to facilitate alignment and stability. All other components could be moved into or out of the laser beam path in a matter of seconds. A second light source, a 6.0-V tungsten lamp, was used exclusively as a broad field background light. The intensity was controlled with a neutral filter and the unattenuated intensity at the eye was 6,500 lux.

Impulse stimuli were generated with the shutter driven by a fast relay circuit. Impulse intensity was controlled with the neutral density wedge. Sine wave illumination was delivered via the ferroelectric modulator with a maximum transmittance of 16%. The modulator was operated as a variable chopper at 500 Hz. Within each 2-ms cycle the duration of the high transmittance phase was continuously varied under voltage control from 2 to 98% of the cycle period. The modulator's sinusoidal response was monitored with a silicon photodiode and the mean intensity was controlled with a neutral density wedge.

Receptive fields were mapped with impulse or continuous stimuli with displacement controlled by a galvanometric scanner (General Scanning, Inc., Waterton, MA) attached to one of the beam steering mirrors. A signal generator and power amplifier drove a mirror deflection ($< 1°$) with a triangle waveform that moved the beam across the width of the condensing lens. The angular sensitivity profiles were measured with impulse stimuli (10–20 ms duration) at low constant intensity and at angular intervals of 1–2°. The results of six traverses of the field were averaged to compute the mean response at each angle of incidence. The spatial distribution of response magnitudes is referred to as the angular response profile. The relationship between the response and the impulse intensity was measured in the center of the field. The angular sensitivity profile was computed from the angular response profile as the reciprocal of the intensity required to produce a constant criterion response at each angle of incidence.

To generate a black line against a homogeneous bright background, an additional lens was introduced to broaden the laser beam so as to fill the field of the condenser lens. This procedure reduced the mean intensity 900-fold. A thin wire was mounted on a second scanner,

which moved the wire through the collimated beam and, depending on the wire diameter, generated a vertical black line of 1–2°.

Optical Alignment

Special precautions were taken to center the impaled receptor on the optical axis of the condenser and to place the geometric center of the hemispherical compound eye at the focal point of the condenser lens. The initial alignment was performed with the laser beam attenuated by 4 log units. After centering the eye as close as possible to the optical axis, the steering mirrors and the condenser was adjusted while observing a stimulus slit on the cornea under the microscope. The distance from the eye to the lens was set with a caliper. Cells were impaled as close as possible to the geometric center of the eye and the alignment was assessed with a rough plot of the receptive field. If the cell was more than 10° from the center of the scan the horizontal position of the condenser lens and one of the steering mirrors was adjusted to align the beam closer to the axis of the receptor.

Data Acquisition and Analysis

Receptor signals were digitized with an a/d converter (model 2801a; Data Translation, Marlboro, MA) in an IBM PC. The sample rate was 100–2,000/s depending on the resolution and length of the record required. Signal averaging was routinely used to obtain reliable estimates of response waveforms. For the smallest signals, up to 200 responses were averaged. All of the receptor potentials considered in the Results are averaged waveforms.

Fourier transforms provide an objective description of the response to sinusoidal stimulation. Both signal averaging and Fourier analysis was performed with a commercial data analysis program, Asystant (Asyst Software Technology, Rochester, NY). Since the program's fast Fourier transform (FFT) algorithm is restricted to 4,096 data points, the sampling rate was adjusted so as to acquire a minimum of 10 sinusoidal response cycles in 4,096 points. Before analysis the average signal amplitude (i.e., the d.c. offset) was subtracted so that the mean signal amplitude was zero.

The parameters of a linear model were estimated by a Gauss–Newton curve-fitting routine (Asystant) applied to the impulse response and the spectral data. The parameter values presented in the Results are those associated with the least-square error.

Stationarity was monitored throughout each experiment. The principal nonstationarity is a slow decline in sensitivity (time scale of 10 s to several minutes) associated with light adaptation (Glantz, 1972; Thorson and Biederman-Thorson, 1974). In addition, receptors are prone to short-term sensitivity changes in either direction (time scale of seconds to 1 min) after transient responses (Hanani and Hillman, 1976; Grzywacz et al., 1988). Both of these phenomena were observed in the unaveraged data. An essential measurement in this study was the impulse response at near-threshold intensity. Nonstationarities in these responses were minimized by adequate separation of successive stimuli and by eliminating the first two or three responses in a train from the subsequent analysis. For the frequency analysis, a reference stimulus (0.6 Hz) was inserted into the sequence of varied stimulus frequencies at several points and small sensitivity shifts were corrected by interpolation. If the sensitivity shifted by more than 50%, the entire sequence was repeated.

As noted above, angular sensitivity profiles were measured with a light bar with a Gaussian intensity profile and a width of 1.6° at half intensity. This stimulus overestimates the width of the narrowest sensitivity profiles. The error calculated by convolution varies from 22% for a 2.5° acceptance angle to $<1.0\%$ for an 8° acceptance angle. The angular sensitivity data were corrected accordingly. The effect of this correction was only significant for the smallest fields, where it reduced the average acceptance angle by 10% (from a measured value of 3.0° to 2.7°).

RESULTS

Fig. 1 summarizes some of the principal features of the crayfish retinular cell impulse response. The response amplitude can exceed 60 mV and varies with intensity over a 4–5 log unit range (Fig. 1 *A*). At the lowest stimulus intensities (Fig. 1 *B*) the response amplitude is linearly related to the light intensity; i.e., increasing the intensity fivefold increases the response amplitude from 0.65 to 3.3 mV. Significant departures from linearity are generally observed for responses that exceed 5–10 mV, or ~10% of the maximum amplitude possible. In Fig. 1 *B* the highest intensity increment is fourfold, but the response increases 2.3-fold (from 3.3 to 7.5 mV). A second general characteristic is that the responses are asymmetric. In dark-adapted cells at the lowest stimulus intensities (Fig. 1 *B*) the rise time (10–90% peak amplitude) is ~40% of the decay time. As the intensity increases, this asymmetry is enhanced such that a 60-mV response arises ~15–20 times faster than it decays (Fig. 1 *A*). Light adaptation disproportionately accelerates the decay phase of the receptor potential and thus diminishes the asymmetry between rising and falling phases (Fig. 1 *C*). In the cell shown, light adaptation (response on left) reduced the sensitivity 250-fold, the time to peak by 50%, and the decay time constant by 67%. In five

FIGURE 1. Impulse responses of crayfish retinular cells. (*A*) Responses of the dark-adapted receptor to a 4.3 log unit range of impulse intensities. Intensity increases in 0.5 log unit steps until the last, which is 0.8 log units. (*B*) Impulse responses of the same cell over a 15-fold range of stimulus intensities (from the bottom up, Log I = −4.4, −4.0, −3.7, and −3.3). (*C*) Impulse response before and during light adaptation. Adaptation reduced sensitivity 250-fold. Scale is 20 mV and 200 ms (*A*); 3 mV and 200 ms (*B*); and 2.5 mV and 100 ms (*C*).

similar measurements, intense light adaptation that diminished sensitivity 2 to 3 log units reduced the average time to peak of the linear response from 83 to 40 ms (i.e., by 52 ± 10%, SD).

Linear Cascades

Fuortes and Hodgkin (1964) proposed that the linear impulse response of *Limulus* receptors can be described by the transfer function of a linear cascade of identical resistor–capacitor (RC) filters. Subsequent studies in *Limulus*, insects, and vertebrates have modified the model to overcome certain discrepancies that are apparent when the cascade is applied to particular cases. These changes include the use of two or more time constants to accommodate the asymmetry of the impulse response (Penn and Hagins, 1972; Baylor et al., 1974) and a fixed delay (DeVoe, 1967; Brodie et al., 1978; Goldring and Lisman, 1983) to accommodate a nonexponential feature of the response. Such a delay could be associated with a diffusion process in the transduction mechanism (Liebman et al., 1987). In the foregoing it is assumed that the response has an absolute delay of 5–10 ms. In linear systems an absolute delay produces a pure phase shift (Milsum, 1966).

In Fig. 2 the continuous traces are averaged impulse responses elicited with a 15-fold range of intensities. In this near-threshold intensity range an eightfold increase in intensity produced a sevenfold increase in response. The broken traces are the impulse responses of a linear cascade described by the equation

$$E(t) = [A/(n-1)!\tau]\,(t/\tau)^{n-1} \exp(-t/\tau) \quad (1)$$

where n is the number of exponential stages ($n = 5$ in Fig. 2) with the same time constant, τ (19 ms in Fig. 2), and A is the amplitude coefficient (proportional to intensity). For a linear cascade the time to peak (t_p) is equal to $\tau(n-1)$. If τ of Eq. 1 is set equal to the measured $t_p/(n-1)$ and n is determined by the least-square error, then the calculated responses both rise and, after a delay, decay more rapidly than the receptor potential. Conversely, a least-square error fit for both n and τ results in a waveform with a t_p that exceeds that of the impulse response by $\sim 10\%$. This pattern of deviations between the receptor responses and the best approximations of Eq. 1 reflect the previously noted response asymmetry and are characteristic of results in most of the 17 other cells so examined.

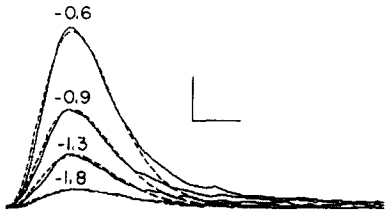

FIGURE 2. Impulse responses (*continuous traces*) approximated by a fifth order linear cascade (Eq. 1, $n = 5$; $\tau = 19$ ms). Log stimulus intensities are indicated above each trace. Scale is 2 mV and 50 ms.

Sine Wave Responses

When the light-adapted photoreceptor is stimulated with sine wave–modulated illumination, the output is approximately sinusoidal over the frequency range of 0.1–25 Hz. Fig. 3 (left column) is a series of responses to sine-modulated illumination from 0.29 to 25 Hz. At the lowest frequencies the peak-to-peak response amplitudes are 1.0–10 mV and the phase typically lags the input by 1–5°. By 1.0 Hz the amplitude has declined measurably and a substantial phase shift (−30 to −40°) is apparent. Between 1.0 and 25 Hz the amplitude declines by 95–99% and the phase shift increases to about −500°. At the highest frequencies there is generally evidence of harmonic distortion. In general, fast Fourier transforms (FFTs) of the sinusoidal responses (Fig. 3, right column) indicate modest harmonic distortion at the very lowest (≤ 0.5 Hz) and highest (≥ 20 Hz) frequencies and virtually none between these frequencies.

The peak-to-peak amplitude of the sinusoidal response is linearly related to the modulation depth (Fig. 4, *A* and *B*) and the phase of the response is independent of modulation depth at all frequencies. In Fig. 4, *A* and *B*, the signal average was referenced to the stimulus sine wave at +90°. Thus, the phase of the 0.6-Hz response was about −34° (Fig. 4*A*) and that of the 3.0-Hz response was about −150°. The results were examined with the FFT. At each stimulus modulation depth the response amplitude was estimated from the Fourier coefficient of the fundamental. Response

amplitude as a function of modulation depth is shown in Fig. 4 *C*. The solid lines are least-square regressions and the slopes reflect the difference in attentuation at the two frequencies. In Fig. 4 *D* the results of four similar experiments were normalized to their amplitudes at maximum modulation. The straight line indicates linearity and the mean square deviation from linearity is 3% of the expected linear value.

Since the sine wave and impulse responses are approximately linear, a comparison was made of the parameters (n, τ) that provides the best estimates (minimum [error]^2)

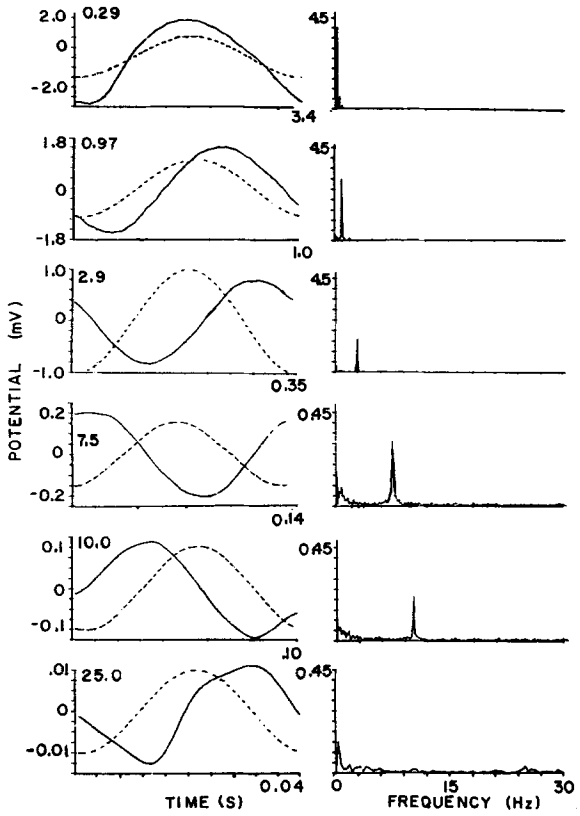

FIGURE 3. Steady-state average sine wave responses and their FFTs. The solid traces in the left column are signal-averaged waveforms (n = 10 at 0.29 Hz and 200 at 25 Hz). Broken traces indicate stimulus phase. The time scale for each panel is the stimulus period in seconds and the vertical scale is adjusted for the signal amplitude as indicated from ±2.0 mV to ±10μV. Right-hand column shows FFTs. The vertical scale is in millivolts and the sensitivity is increased 10-fold at 7.5 Hz. Horizontal scale is 0–30 Hz throughout.

of the observed waveforms. The frequency response of a linear cascade is:

$$E/E_0 = [1 + (2\pi F\tau)^2]^{-n/2} \tag{2}$$

where E_0 is the low frequency sine response amplitude and F is the frequency in Hz. The phase (P) of the response is given by:

$$P = -D2\pi F - \text{nARCTAN}\,(2\pi F\tau) \tag{3}$$

where D is a fixed delay.

Fig. 5 *A* is an impulse response (continuous trace) at a just suprathreshold intensity and the response of a fourth order cascade, Eq. 1 (broken line), with τ = 29 ms. Fig. 5, *B* and *C* (filled circles), are the amplitude and phase, respectively, of the sine wave

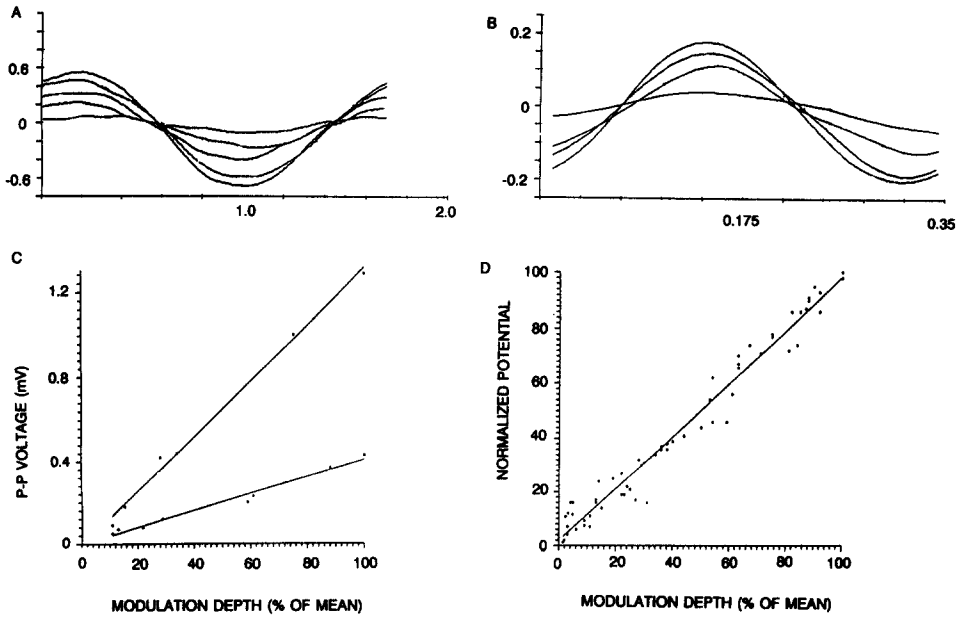

FIGURE 4. Effect of modulation depth on sine wave response amplitude and phase. (*A*) Averaged responses to 0.6-Hz stimuli at ±5 to ±95% modulation. Axes are labeled in millivolts and seconds. (*B*) Averaged responses to 3.0-Hz stimuli from ±10 to ±95% modulation. (*C*) Response amplitude as a function of modulation depth for the cell in *A* and *B*. The straight lines are linear regressions. The upper and lower functions are for 0.6 and 3.0 Hz, respectively. (*D*) Response amplitude versus modulation depth for 0.3-Hz stimulation. Normalized results from four cells are shown.

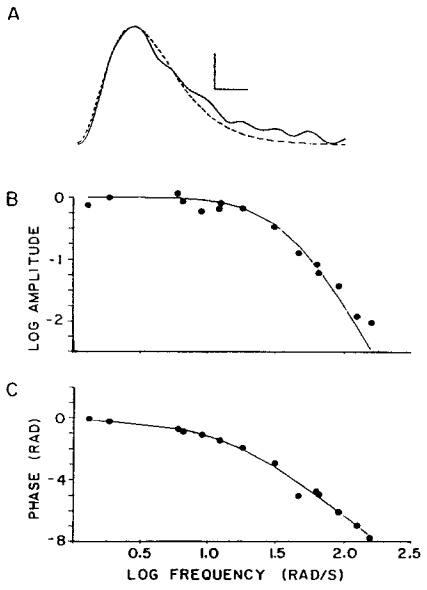

FIGURE 5. Impulse and frequency response of receptor described by a fourth order linear cascade. (*A*) Impulse responses of receptor (*solid lines*), Log $I = -2.7$. The response is approximated by a fourth order function with $\tau = 29$ ms (*broken line*). Scale is 0.2 mV and 50 ms. (*B*) Log of relative sine response amplitude vs. log frequency (radians per second). Symbols are data points derived from FFTs. Low frequency peak-to-peak amplitude is 4.0 mV. Continuous traces in *B* and *C* are the responses of a fourth order cascade with $\tau =$ 26 ms. (*C*) Phase vs. log frequency.

response. These data are well described by Eqs. 2 and 3 (continuous lines in Fig. 5, *B* and *C*) with $n = 4$, $\tau = 26$ ms, and $D = 5$ ms. Thus, the frequency response can be described by a transfer function of the same order as the impulse response, but the τ of the impulse response is 10–15% greater than that of the frequency response. A small discrepancy between the two estimators of τ was common among 16 such cases examined and probably reflects a modest shift in the degree of adaptation between the two measurements. Among the 16 such cases examined, the order (n) varied between three and five and the higher values of n were generally associated with the most light-adapted cells. In Fig. 5, and in most of the receptors examined, the linear cascade model provided a better description of the frequency response than of the impulse response (by the criterion of least-square error relative to mean signal amplitude).

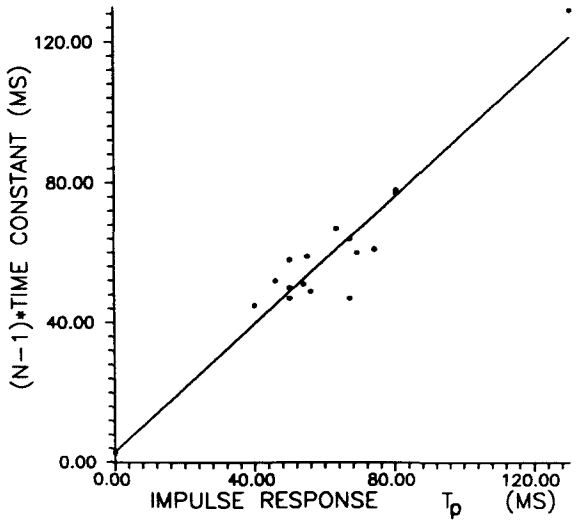

FIGURE 6. Correlation of impulse response time to peak (t_p) and the time constants for the best-fitting linear cascade model of the frequency response for 15 cells. The solid line is the linear regression $(n - 1)\tau = 0.93\ (t_p) + 2.9$ ms. The correlation coefficient is 0.95.

Since the t_p for the cascade's impulse response is $\tau(n - 1)$, one can compare the t_p predicted from frequency analysis and the observed t_p of the impulse response for cascades of all orders. The results in Fig. 6 reveal the discrepancy noted above (the slope of the least-square regression is 0.93) but also indicate a strong relationship between the two estimates of τ (correlation coefficient, $r = 0.95$ for $n = 16$). With the exception of a single data point the t_p values are clustered between 40 and 80 ms, which is similar to the range of values for impulse responses measured in light- and dark-adapted conditions, respectively.

Contrast Sensitivity

Previous studies in crayfish receptors (Glantz, 1972) demonstrated that when a flash is superposed on a steady background, the incremental sensitivity declines but the contrast sensitivity increases as the background intensity increases (over five orders of magnitude). Specifically, the threshold intensity, I, for any arbitrary response in the

presence of a steady background light I_b is:

$$I = kI_b^m \tag{4}$$

where m is a constant ranging from 0.55 to 0.73 and k is proportional to the criterion response amplitude. If the threshold contrast is I/I_b, then the contrast sensitivity, C, is proportional to its inverse, I_b/I, and from Eq. 4:

$$C = I_b/I = I_b/kI_b^m = I_b^{1-m}/k \tag{5}$$

where C is a dimensionless variable. Eq. 5 states that the response to a given percent change in mean intensity will increase as the 1-m power of the mean intensity. Fig. 7 shows the effect of increasing the mean intensity on the sinusoidally driven response while maintaining a constant percent modulation. A 100-fold increase in mean intensity (+) produces a 5.0-fold increase in the peak-to-peak response amplitude. It should also be noted that the higher intensity reduces the absolute sensitivity ~20-fold and the time constant by 40%. In similar experiments, 10- and 100-fold increases in the mean intensity produced 85 ± 10% (SD, n = 6) and 320 ± 20%

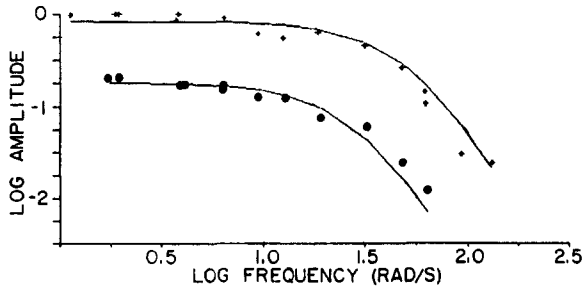

FIGURE 7. Relative response amplitude as a function of frequency for two mean intensities (log $I = -1.1$ [*crosses*] and log $I = -3.1$ [*filled circles*]) at the same percent modulation (±95%). The response amplitudes were normalized to the amplitude of the low frequency response (1.65 mV) at the higher intensity. The continuous functions are from Eq. 2 with n = 4 and τ = 31.7 ms (lower function) and τ = 17.5 ms (upper function).

(n = 3) increases in contrast sensitivity, respectively. For these conditions, Eq. 5 with m of 0.7 predicts increases in contrast sensitivity of 99 and 298%, respectively. Qualitatively similar results are described in a wide variety of photoreceptors (DeVoe, 1985), including *Limulus* and locusts (Pinter, 1966, 1972), flies (Laughlin et al., 1978, 1987; Dubs, 1982; Howard et al., 1984, 1987), and turtle cones (Naka et al., 1987).

Spatial Properties

The angular sensitivity profile is determined by the physical properties of the dioptric apparatus (ommatidium), the dimensions of the receptors, and the state of adaptation (Land, 1984). Fig. 8*A* is a sample of two such profiles from moderately dark-adapted receptors. The acceptance angles (angular widths at 50% maximal sensitivity) for these receptors are 11 and 6.8°. A sample of 12 such cells exhibited acceptance angles of 6.0–12° with a mean of 8.8 ± 0.6° (SE). The shape of the profile is approximately Gaussian (broken lines in Fig. 8*A*). During light adaptation, screening pigments reduce the acceptance angle toward a minimum determined by the interommatidial angle. Previous measurements (Shaw, 1969) indicate that excised

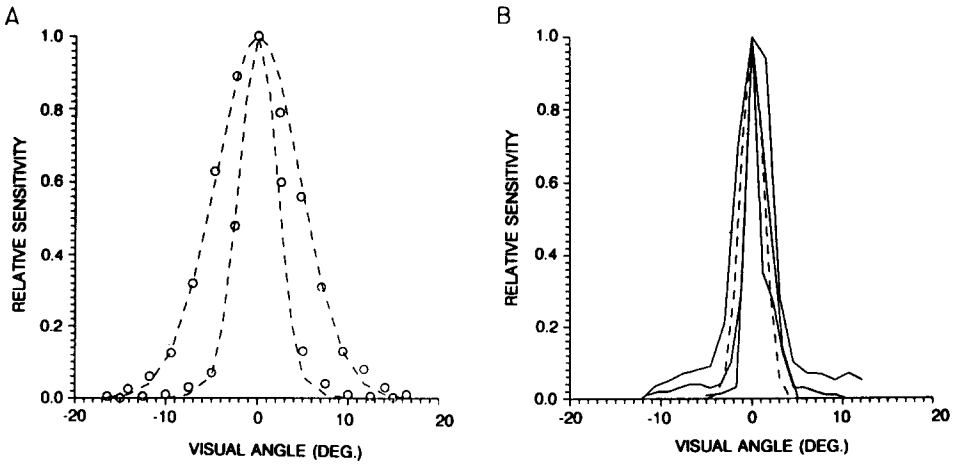

FIGURE 8. (*A*) Angular sensitivity profiles for two receptors in dark-adapted preparations. The acceptance angles for these cells are 6.8 and 11°. The broken traces are Gaussian functions. (*B*) Angular sensitivity profiles of three receptors from excised eyes. Acceptance angles are 1.7, 3.3, and 4.8°. The broken line is a Gaussian with a 3.0° acceptance angle.

eyes obtain this minimum. In Fig. 8 *B* the solid lines are sensitivity profiles of receptors from three excised eyes with acceptance angles of 1.7, 3.3, and 4.8°. The mean for seven such cells was 2.7 ± 0.6° (SE). The dashed line is a Gaussian with a 3° acceptance angle. Although the shape of the profile is approximately Gaussian (Bryceson and McIntyre, 1983), many receptors exhibit a broad skirt of higher than Gaussian sensitivity at large angular deviations (Dubs, 1982; Smakman et al., 1984).

For impulse intensities in the linear range, the normalized angular sensitivity and angular response profiles are identical. The smooth continuous function in Fig. 9 *A* is an angular response profile elicited by impulse stimuli at successive adjacent locations 1.6° apart. The intensity was adjusted so that the maximum response (4.8 mV) was in the linear range and the stimulus diameter was 1.6°. The angular width at half-maximal response was 5.6°. When the sensitivity at each position is determined

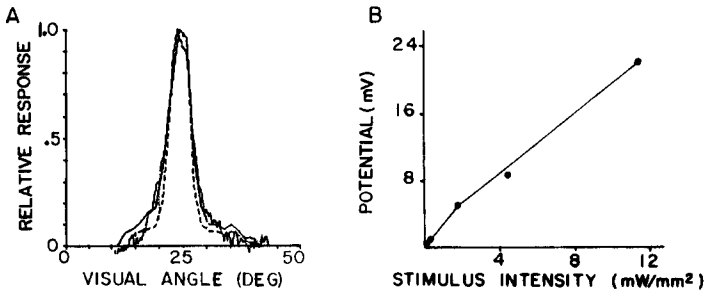

FIGURE 9. (*A*) Comparison of angular response (*smooth and noisy solid lines*) and sensitivity (*broken line*) profiles for a receptor probed with a low intensity impulse stimulus and a continuous scan of the field at 10.1°/s. Peak response amplitude was 4.8 mV. (*B*) Impulse response amplitude versus stimulus intensity. Each point is the average of 10 responses.

from the response intensity function in Fig. 9 *B*, the angular sensitivity profile (broken line) exhibits an acceptance angle of 5.1°. An important feature of the angular sensitivity profile is that it is independent of stimulus intensity (Cornsweet, 1970) and is related to the physical properties of the optical pathway (Smakman et al., 1984).

Almost hidden in Fig. 9 *A* is an angular response profile generated by a continuous scan of the same cell (with the same stimulus) at a low velocity (10.1°/s). The shapes of the two angular response profiles are quite similar and the angular widths at 50% peak amplitude are identical. The profile produced by a continuous scan has the added feature that it is a time domain signal that provides a good approximation of the angular sensitivity profile.

Velocity Sensitivity

When a narrow bar of light moves across the field of a receptor, the output of the receptor reflects the action of two concatenated filters: a spatial filter such as those described by Figs. 8 and 9, and a purely temporal filter as approximately by the impulse response. If the width of the stimulus is small compared with the acceptance angle, and the angular sensitivity profile is $f(x)$, then the effective stimulus ($I(t)$) produced by a constant velocity angular movement, $s = (x/t)$, of a linear range intensity is:

$$I(t) = f(st) \tag{6}$$

If the system is linear, the convolution of the impulse response and the time domain representation of the angular response profile should be able to predict the response to the scanning bar at all velocities. To perform this calculation, changes in stimulus velocity were simulated by a linear compression of the time base of the angular response profile. Typically, a scan of 48° is made at 10°/s and requires 4.8 s for its completion. A simulated input scan at 100°/s is represented as the identical angular response profile, but is distributed over 0.48 s. For a Gaussian sensitivity profile with acceptance angle ϕ and stimulus velocity s, the effective stimulus is:

$$I(t) = I \exp\left[(-\ln 2)(2st/\phi)^2\right] \tag{7}$$

Fig. 10 (upper left) is the response to a 9.5-s back and forth scan of a 48° arc with a linear range stimulus intensity. Adjacent to it is the impulse response at the intensity of the scanning bar. The solid traces in the remaining panels of Fig. 10 are averaged responses of the receptor to successively faster scans from 31 to 1,067°/s. The broken traces are the responses calculated by the convolution of the impulse response and the angular response profile. The vertical scale is expanded (for clarity) as the velocity is increased. The width of the horizontal axis is always the time occupied by a 48° scan in each direction. As the velocity increases, the amplitude declines and the phase lag increases. At the highest velocity the measured signal amplitude has declined to ~100 μV (i.e., by 98%) and the angular phase has shifted by −53°. Furthermore, between 100 and 200°/s the form of the response changes from that of the dynamic angular response profile to the asymmetric form of the impulse response. The convolution is an excellent predictor of all these changes. It

should be noted, however, that the results in Fig. 10 describe the receptor's velocity sensitivity for a particular angular response profile and impulse response.

Because this receptor is linear for modulations on either side of the mean intensity, the response to a moving black stripe should be predictable from the convolution of the sensitivity profile and a negative impulse response (Fig. 11). In this instance the low velocity scan (9.6°/s) elicited a response of −1.3 mV. At 716°/s the amplitude is −40 μV (32-fold attenuation) and the angular phase lag is −40°. Thus, the velocity-dependent attentuations of negative and positive responses are similar and predictable from the separate spatial and temporal transfer functions. In both, the relation between attenuation and velocity implicitly depends on the receptor's time constant and acceptance angle.

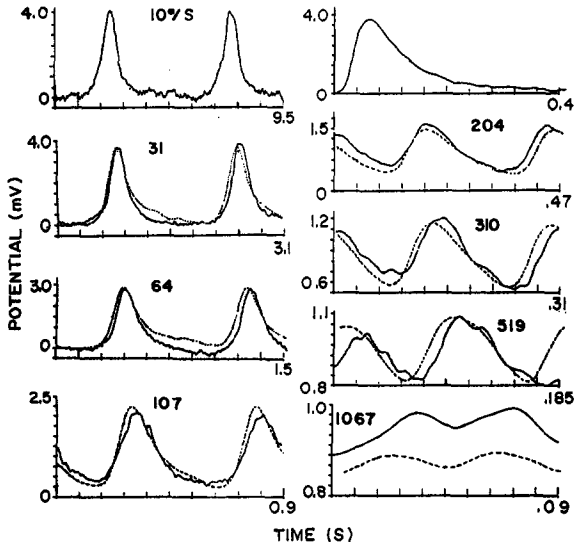

FIGURE 10. Receptor responses to the oscillating motion of a bright bar at varying velocity. Each receptor potential (*solid traces*) is the average of 10 (10°/s) to 100 (1,067°/s) responses. The vertical scale is adjusted from 4.0 to 0.2 mV to accommodate the variations in response amplitude. The horizontal scale is equal to the period of one stimulus cycle. For each panel the stimulus traversed 48° in the horizontal plane in each half cycle. The upper right panel shows the impulse response elicited with the same intensity as the scanning line (log I = 0). The broken traces are produced by convolution of the impulse and the angular response profile measured at 10°/s. Note that above 300°/s the voltage scales have a nonzero reference.

The above analysis also depends on an assumed constant velocity stimulus motion and the linearity of the stimulus–response relationship. We also observed, however, that the spatiotemporal convolution yielded excellent predictions of response amplitude and phase for stimuli up to a log unit above the linear range. This implies that the calculated velocity-dependent response attenuation can withstand a modest nonlinearity in the impulse response. At still higher intensities, the angular response profile is much broader than the angular sensitivity profile and the convolution provides an inferior approximation of response amplitude and phase at high velocities.

The simplest model of the receptor's linear spatiotemporal performance is obtained if we assume that the dynamic transfer function is adequately described by a linear cascade of order n, with a single time constant (τ) and a Gaussian angular sensitivity profile with acceptance angle ϕ. When this system is presented with a

narrow bar of light of a fixed linear range intensity, the sensitivity to any constant angular velocity is entirely specified by τ and ϕ. The time course of the response, $E(t)$, can be derived by convolution of the time domain transfer function (Eq. 1) and the Gaussian sensitivity profile (Eq. 7):

$$E(t) = A[\tau(n-1)!]^{-1}(t/\tau)^{n-1}e^{-t/\tau} * e^{-\ln 2(st/\phi)\wedge 2} \quad (8)$$

where the asterisk stands for convolution. For a given receptor in a stationary

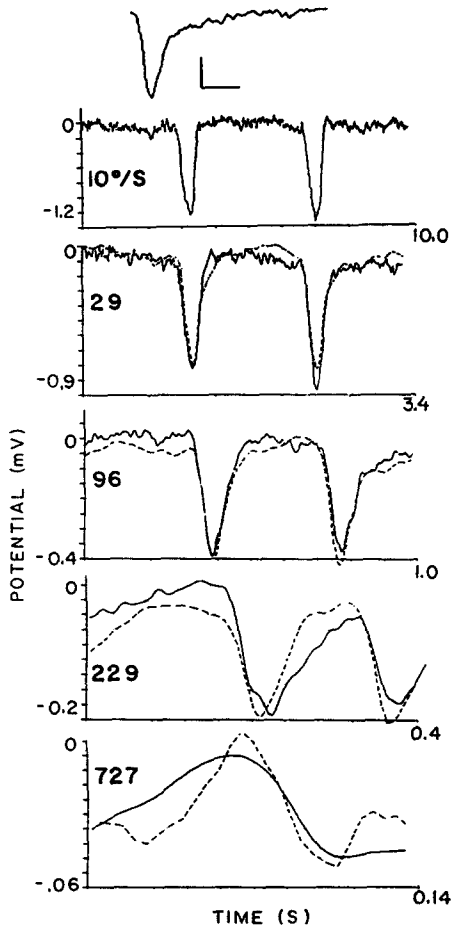

FIGURE 11. Receptor responses to the oscillating motion of a black line against a homogeneous background (log $I = -3.0$). The top trace is the negative impulse response (log I from -3.0 to -5.0 for 20 ms). Scale is 0.1 mV and 100 ms. Responses to moving bar are averaged and scaled as in Fig. 10. Target velocity is indicated at the left in each panel. Broken traces are the result of convolving the negative impulse response (*top trace*) and the 10°/s scan.

adaptive state, τ and ϕ are assumed to be constant and time (t) and velocity (s) are the only variables.

The convolution was solved numerically using time increments of 1 ms and angular increments of 1°. For each combination of ϕ and τ values the peak value of $E(t)$ was obtained for stimulus velocities over the range of 1–1,000°/s. The calculated peak response amplitudes were then normalized with respect to the largest such response to yield the relative response amplitudes. In Fig. 12 *A* the calculated relative response

amplitude is plotted as a function of the stimulus velocity for the physiological range of τ and ϕ. The calculations indicate that: (*a*) Changes of a given percent in ϕ or $1/\tau$ have identical effects on the velocity-dependent response. Each curve in Fig. 12 *A* is a velocity–response profile for a given ratio of ϕ/τ (which has the dimension of an angular velocity in degrees per second). Curves *a–e* represent successive doublings of ϕ/τ from 25 to 400°/s. Thus, curve *d* is the velocity sensitivity profile for ϕ/τ of 200°/s (i.e., $\phi = 5°$, $\tau = 25$ ms; $\phi = 10°$, $\tau = 50$ ms; etc.) (*b*) The velocity of the half-maximal response (v_s; broken line in Fig. 12 *A*) is a linear function of ϕ/τ. (*c*) Beyond a certain velocity the response declines linearly with velocity for all values of ϕ/τ; i.e., the slope on the log–log plot is -1. This is due to the fact that at high velocities the stimulus

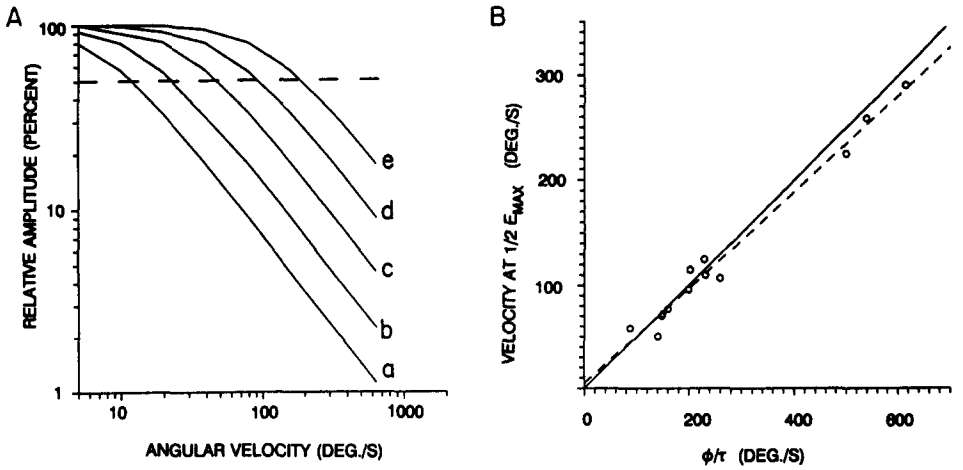

FIGURE 12. Calculated and measured velocity sensitivities for various response time constants and acceptance angles. (*A*) Calculated response amplitude vs. angular velocity based on Eq. 8 and assuming a temporal transfer function of a third order cascade and Gaussian sensitivity profile. In curves a–e the value of ϕ/τ increases successively by a factor of 2 from 25 to 400°/s. (*B*) The velocity of the half-maximal response as a function of $\phi.\tau$. The solid line is derived from Eq. 8 for receptors with third order dynamics. The open circles are the results from 13 receptors in a wide range of adaptive states, all treated as though they exhibited third order dynamics for the purpose of comparison. The broken line is the least-square for the measured values and has a slope of 0.46.

approximates an impulse with power (time integral of $I(t)$), which declines linearly with velocity. (*d*) Changes in n (the order of the linear cascade) of Eq. 8 have only modest effects on the velocity-dependent response. Thus, increasing n from 3 to 4 reduces v_s by 16% and shifts the linear portion of the function by the same amount along the horizontal axis. This minimal effect is due to the conditions described above in (*c*) and contrasts with the important effects of n on the frequency response where the asymptotic log–log slope is $-n$.

Although it is not indicated in Eq. 8, it should be noted that increasing the contrast sensitivity (C) for constant ϕ and τ shifts the velocity–response function upward along the vertical axis by the difference in C. Thus, a 10-fold increase in mean intensity

doubles C (for $m = 0.7$ in Eq. 5), which in turn doubles $E(t)$ for any combination of ϕ, τ, and velocity. The shape of the velocity–response profile does not change, but for a given increase in C the response to any velocity will be greater by ΔC-fold, and for a given response amplitude the associated velocity will increase linearly with C.

In Fig. 12 *B* the solid line is the calculated velocity of the half-maximal response (for a third order cascade) as a function of ϕ/τ and has a slope of 0.5. The open circles are the measured half-maximal velocities of 13 receptors similar to those in Figs. 10 and 11. Within this population τ varied from 15 to 60 ms, ϕ varied from 3.5 to 10°, and the contrast sensitivity varied over a sevenfold range. For the sake of this comparison, all 13 cells are treated as though they exhibited third order dynamics and τ was estimated from $t_p/(n - 1)$. The broken line is the least-square regression of the measurements with slope of 0.46. The modest discrepancy between the data and the theoretical function is principally due to the fact that n actually varies between 3 and 5 and the temporal functions only approximate the assumptions of Eq. 8. Given this reservation, Eq. 8 provides a simple and useful framework for the analysis of receptor responses to moving targets.

DISCUSSION

The dynamic properties of crayfish retinular cells are similar to those of other arthropods and also share important characteristics with vertebrate receptors. Between threshold and saturation, the sensitivity declines ~250-fold and the rise and decay times diminish significantly. During light adaptation a 250-fold decline in sensitivity is associated with a 50% decline in the time to peak. A virtually indentical result in *Limulus* eccentric cells prompted Fuortes and Hodgkin (1964) to propose a linear cascade model of phototransduction. In this scheme the time constant is proprotional to an analogue resistance, R, while the sensitivity is determined by R^n where n is the number of identical RC segments in the cascade. Thus, an eighth order cascade could in principle accommodate the adaptation-dependent changes of the crayfish receptor's impulse response. The impulse response time course, however, was far too asymmetrical for an eighth order model. For impulse intensities within 1.5 log units of threshold and response amplitudes <5 mV (the linear range), the intensity-dependent shifts in time scale and sensitivity are small (typically $<10\%$) and the responses can be described by a time-shifted third to fifth order linear cascade. The only discrepancy is that the higher order cascades provide the best fit to the S-shaped rising phase, but decay more rapidly than the measured response. Similar discrepancies have been documented in both arthropod (Pinter, 1972; French and Jarvilehto, 1978) and vertebrate (Penn and Hagins, 1972; Baylor et al., 1974) receptors.

The sine wave responses are dominated by the fundamental over the entire frequency range examined (0.1–25 Hz), but some harmonic distortion is observed at the extremes. Similar characteristics are described for *Limulus* (Pinter, 1966) and fly (Dubs, 1982) receptors. As expected for a linear system, the sinusoidal response amplitude varies linearly with modulation depth while the phase is invariant. Between 0.1 and 25 Hz the sine response amplitude and phase exhibit the low-pass behavior of a linear RC cascade. In this regard the crayfish retinular cell resembles those of cricket (Pinter, 1972) and fly (French and Jarvilehto, 1978), in contrast to the

pronounced band-pass behavior of *Limulus* (Pinter, 1966; Dodge et al., 1968), locust (Pinter, 1972), spider (DeVoe, 1967), and turtle cones (Naka et al., 1987).

In a linear system the transfer function specifies the response to sinusoidal inputs. This relationship was examined in 16 cells through a comparison of the calculated and measured sine wave response amplitude and phase. The dynamic responses are well described by a linear cascade transfer function of the same order as the impulse response and similar τ. The converse of the above procedure is to specify the impulse response time course from the inverse Fourier transform of the frequency response. This procedure yields a rough approximation of the impulse response in cricket and locust retinular cells (Pinter, 1972) and of the electroretinogram in spiders (DeVoe, 1967).

Because the crayfish has a superposition compound eye, the light impinging on a single receptor is transmitted through a varying number facets (Shaw, 1969). The aperture is determined by the position of screening pigments, which migrate under the control of light and hormones along the partition separating the ommatidia. In the crayfish *Procambarus clarkii,* light adaptation reduces ϕ from $\sim 8.8°$ to $2.7°$ (3.2-fold). The minimum ϕ is less than that of the Australian crayfish (*Cherax destructor*), which is $\sim 4°$ (Bryceson and McIntyre, 1983) and about twice that of the dipteran apposition eye (1.2–2.1°) (Hardie, 1979; Dubs, 1982; Smakman et al., 1984).

The angular sensitivity profile plays an essential role in movement detection. For movements of a narrow stimulus of fixed contrast and at a given angular velocity, the angular sensitivity profile determines the time course of the effective stimulus. As the acceptance angle increases (for a Gaussian angular sensitivity profile), both the rise time and the duration of stimulus action will increase. Thus, for a given receptor time constant, the angular sensitivity profile determines the range of detectable velocities.

An important and general aspect of visual function is the trade-off between sensitivity and acuity as the visual system adapts to changing levels of ambient illumination. In compound eyes, light adaptation alters all of the retinular cell parameters that determine the sensitivity to a moving target: ϕ, τ, and the contrast sensitivity, C. It is possible that movement sensitivity has played an important role in the evolution of the various strategies for coping with changes in ambient illumination. Because contrast sensitivity is generally greater at higher levels of illumination (Eq. 5), most photoreceptors exhibit a performance enhancement as the mean intensity increases (Table I). Adaptation-dependent changes in ϕ and τ may augment or counter this enhancement. During dark adaptation ϕ and τ increase along with the incremental sensitivity. If, however, τ increases by a substantially greater proportion than ϕ, it will diminish the range of detectable velocities. In arthropods the adaptation-dependent changes in receptor time constant and acceptance angle tend to move in parallel, which minimizes adaptation's effect on the velocity sensitivity profile (Table I). In a fully dark-adapted crayfish eye the acceptance angle is ~ 3.2 times that of the light-adapted eye, and the receptor time constant is 2.1 times greater. Thus ϕ/τ increases by $\sim 50\%$ with dark adaptation and this partially offsets the substantial (76%) loss of contrast sensitivity at lower light levels. This would appear to be an appropriate adaptation for movement detection by a nocturnal animal.

For the purpose of comparison, ϕ and t_p are tabulated for several arthropod and turtle receptors (Table I). The value derived for v_s is predicated on the assumption that the temporal dynamics of these receptors is sufficiently similar to that of crayfish so that ϕ/τ provides a rough approximation of their velocity sensitivity. Since contrast sensitivity is enhanced by high light levels in all of these species, I will focus on variations in ϕ/τ. In the apposition eye of *Limulus*, the limiting values of ϕ and τ precisely offset one another (Table I). Thus, *Limulus* velocity sensitivity should be relatively independent of light adaptation. In the locust, the detectable velocity range increases by 50% with light adaptation (Table I). In these arthropods, as in crayfish, adaptation has a much smaller effect on ϕ/τ than on ϕ or τ taken alone. Flies that are generally diurnal provide an interesting exception. They have both the smallest acceptance angles and the fastest responses among the arthropods. In *Calliphora*, light adaptation reduces ϕ by only 20% (Hardie, 1979; Smakman et al., 1984), while reducing τ by 67% (Jarvilehto and Zettler, 1971; Howard et al., 1987). Thus, for dipteran receptors, the range of detectable velocities should increase by ~2.5-fold

TABLE I

The Parameters of Linear Velocity Sensitivity at Low and High Levels of Ambient Illumination in Arthropod and Turtle Photoreceptors

	Low light			High light			
	ϕ	t_p	v_s	ϕ	t_p	v_s	C
	deg	*ms*	*deg/s*	*deg*	*ms*	*deg/s*	
Crayfish	8.8	83	106	2.7	40	68	4.2
Limulus*	12.3	116	106	6.0	55	109	2.5
Locust‡	2.4	48	50	1.5	20	75	2.2
Fly§	1.5	25	60	1.2	8.3	145	4.0
Turtle‖	0.75	40	19	0.75	20	38	2.2

*t_p from Fuortes and Hodgkin (1964), ϕ from Barlow et al. (1980), C from Pinter (1966). ‡t_p from Payne and Howard (1981), ϕ from Wilson (1975), C from Pinter (1972). §t_p and S_c from Howard et al. (1987), ϕ from Smakman et al. (1984). ‖From Naka et al. (1987).

with strong light adaptation. This was shown behaviorally by Pick and Buchner (1979).

For the purpose of comparison, the parameters relevant to linear velocity sensitivity in turtle cones are provided in Table I. The high acuity of the turtle's retinal mosaic exacts a severe penalty with respect to movement detection. Dark adaptation slows the receptor dynamics but does nothing for the acceptance angle. Other things being equal, the range of detectable velocities of a dark-adapted turtle cone is less than half that of most arthropods. It should be noted that the acceptance angle of turtle cones is substantially enlarged (relative to isolated cones) by electrotonic coupling among receptors (Baylor et al., 1974; Copenhagen and Green, 1987). It is possible that the requirements of movement detection provide a selective pressure for electrotonic coupling among photoreceptors (and the associated sacrifice of acuity).

The full significance of the above analysis can only be assessed in the context of a model of the neuronal basis of velocity sensitivity. From the perspective of current

models, however, it is clear that photoreceptor dynamics should determine the upper end of the detectable velocity range (Buchner, 1984; Egelhaaf and Borst, 1989). In crayfish optokinetic motoneurons (Wiersma and Oberjat, 1968), sensitivity to a moving stripe is constant from 0.1 to 24°/s and declines to about half-maximum at 100°/s and to zero by 280°/s. This profile is in general accord with the results in Fig. 12 *B* and Table I. In low light levels the movement-elicited response is ~35% that at the higher intensity. This result is predictable from the data in Table I, where the lower light level is associated with a 56% larger v_s (106/68) but only 24% of the contrast sensitivity (1/4.2) compared with that at the higher light level. Thus, the expected response at low light levels is ~37% (0.24 × 1.56) that observed at the higher intensity.

I thank Dr. Harvey Nudelman of Baylor College of Medicine, who provided important advice at numerous points in this investigation, and I also thank Dr. Nudelman and Dr. John Clark of Rice University for their useful critical comments on this manuscript.

These studies were supported by National Science Foundation grant BNS-8711141.

Original version received 21 May 1990 and accepted version received 9 November 1990.

REFERENCES

Barlow, R. B., S. C. Chamberlain, and J.-Z. Levinson. 1980. Limulus brain modulates the structure and function of the lateral eyes. *Science.* 210:1037–1039.

Baylor, D. A., A. L. Hodgkin, and T. D. Lamb. 1974. The electrical response of turtle cones to flashes and steps of light. *Journal of Physiology.* 242:685–727.

Brodie, S. E., B. W. Knight, and F. Ratliff. 1978. The spatiotemporal transfer function of the *Limulus* lateral eye. *Journal of General Physiology.* 72:167–202.

Bryceson, D. P., and P. McIntyre. 1983. Image quality and acceptance angle in a reflecting superposition eye. *Journal of Comparative Physiology.* 151:367–380.

Buchner, E. 1984. Behaviorial analysis of spatial vision in insects. *In* Photoreception and Vision in Invertebrates. M. A. Ali, editor. Plenum Publishing Corp., New York. 651–621.

Copenhagen, P. R., and D. G. Green. 1987. Spatial spread of adaptation within the cone network of turtle retina. *Journal of Physiology.* 393:763–776.

Cornsweet, T. N. 1970. Visual Perception. Academic Press Limited, London. 312–354.

DeVoe, R. D. 1967. A nonlinear model for transient responses from light-adapted wolf spider eyes. *Journal of General Physiology.* 50:1993–2030.

DeVoe, R. D. 1985. The eye: electrical activity. *In* Comprehensive Insect Physiology Biochemistry and Pharmacology. G. A. Kerkut and L. I. Gilbert, editors. Pergamon Press Inc., Elmsford, NY. 278–353.

Dodge, F. A., B. W. Knight, and J. Toyoda. 1968. Voltage noise in *Limulus* visual cells. *Science.* 160:88–90.

Dubs, A. 1982. The spatial integration of signals in the retina and lamina of the fly compound eye under different conditions of luminance. *Journal of Comparative Physiology.* 146:321–343.

Egelhaaf, M., and A. Borst. 1989. Transient and steady-state response properties of movement detectors. *Journal of the Optical Society of America.* 6:116–127.

French, A. S., and M. Jarvilehto. 1978. The dynamic behavior of photoreceptor cells in the fly in response to random stimulation at a range of temperatures. *Journal of Physiology.* 274:311–322.

Fuortes, M. G. F., and A. L. Hodgkin. 1964. Changes in time scale and sensitivity in the ommatidia of *Limulus*. *Journal of Physiology.* 172:239–263.

Glantz, R. M. 1972. Visual adaptation: a case of nonlinear summation. *Vision Research.* 12:103–109.

Goldring, M. A., and J. E. Lisman. 1983. Single photon transduction in *Limulus* photoreceptors and the Borsellino-Fuortes model. *IEEE Transactions.* SMC-13:727–731.

Goldsmith, T. H. 1978. The effects of screening pigments on the spectral sensitivity of some crustacea with scotopic (superposition) eyes. *Vision Research.* 18:475–482.

Grzywacz, N. M., P. Hillman, and B. W. Knight. 1988. The quantal source of area supralinearity of flash responses in *Limulus* photoreception. *Journal of General Physiology.* 91:659–684.

Hanani, M., and P. Hillman. 1976. Adaptation and facilitation in the barnacle photoreceptor. *Journal of General Physiology.* 67:235–249.

Hardie, R. C. 1979. Electrophysiological analysis of fly retina. 1. Comparative properties of R1-6 and R 7 and 8. *Journal of Comparative Physiology.* 129:19–33.

Howard J., B. Blakeslee, and S. B. Laughlin. 1987. The intracellular pupil mechanism and photoreceptor signal: noise ratios in the fly *Lucilia cuprina. Proceedings of the Royal Society of London, B.* 231:415–435.

Howard, J., A. Dubs, and R. Payne. 1984. The dynamics of phototransduction in insects. *Journal of Comparative Physiology.* 154:707–718.

Jarvilehto, M., and F. Zettler. 1971. Localized intracellular potentials from pre- and postsynaptic components in the external plexiform layer of an insect retina. *Zeitschrift für Vergleichende Physiologie.* 75:422–440.

Knight, B. W., J.-I. Toyoda, and F. A. Dodge. 1970. A quantitative description of the dynamics of excitation and inhibition in the eye of *Limulus. Journal of General Physiology.* 56:421–437.

Land, M. 1984. Crustacea. *In* Photoreception and Vision in Invertebrates. M. A. Ali, editor. Plenum Publishing Corp, New York. 401–438.

Laughlin, S. B., and R. C. Hardie. 1978. Common strategies for light adaptation in the peripheral visual system of fly and dragonfly. *Journal of Comparative Physiology.* 128:319–340.

Laughlin, S. B., J. Howard, and B. Blakeslee. 1987. Synaptic limitations to contrast coding in the retina of the blowfly *Calliphora. Proceedings of the Royal Society of London, B.* 231:437–467.

Liebman, P. A., K. R. Parker, and E. A. Dratz. 1987. The molecular mechanism of visual excitation and its relation to the structure and composition of the rod outer segment. *Annual Review of Physiology.* 49:765–791.

Milsum, J. H. 1966. Biological Control Systems Analysis. McGraw-Hill Inc., New York. 214–219.

Naka, K.-I., M.-A. Itoh, and R. L. Chappell. 1987. Dynamics of turtle cones. *Journal of General Physiology.* 89:321–337.

Payne, R., and J. Howard. 1981. Response of an insect photoreceptor: a simple log-normal model. *Nature.* 290:415–416.

Penn, R. D., and W. A. Hagins. 1972. Kinetics of the photocurrent of retinal rods. *Biophysical Journal.* 12:1073–1094.

Pick, B., and E. Buchner. 1979. Visual movement detection under light and dark adaptation in the fly *Musca domestica. Journal of Comparative Physiology.* 134:45–54.

Pinter, R. R. 1966. Sinusoidal and delta function responses of visual cells of the *Limulus* eye. *Journal of General Physiology.* 49:565–593.

Pinter, R. B. 1972. Frequency and time domain properties of retinular cells of the desert locust (*Shistocerca gregaria*) and the house cricket (*Acheta domesticus*). *Journal of Comparative Physiology.* 677:383–397.

Shaw, S. R. 1969. Optics of arthropod compound eye. *Science.* 165:88–90.

Smakman, J. G. J., J. H. Van Hataren, and D. G. Stevenga. 1984. Angular sensitivity of blowfly photoreceptors: intracellular measurements and wave-optical predictions. *Journal of Comparative Physiology.* 155:239–247.

Thorson, J., and M. Biederman-Thorson. 1974. Distributed ralaxation processes in sensory adaptation. *Science.* 183:161–172.

Wald, G. 1967. Visual pigments of crayfish. *Nature.* 215:1131–1133.

Wiersma, C. A. G., and T. Oberjat. 1968. The selective responsiveness of various crayfish oculomotor fibers to sensory stimuli. *Comparative Biochemistry and Physiology.* 26:1–16.

Wilson, M. 1975. Angular sensitivity of light and dark adapted locust retinula cells. *Journal of Comparative Physiology.* 97:323–328.